JOURNAL OF CATALYSIS 148, 639–647 (1994)

A Steady-State Tracing Kinetic Analysis of Oxidative Coupling of Methane over Li^+-Doped TiO_2: Mechanistic Aspects of the Carbon and Oxygen Reaction Pathways to Form CO_2

A. M. Efstathiou,* S. Lacombe,† C. Mirodatos,† and X. E. Verykios*

*Institute of Chemical Engineering and High Temperature Chemical Processes, Department of Chemical Engineering, University of Patras, GR-26500, Patras, Greece; and †Institut de Recherches sur la Catalyse, 2 Avenue Albert Einstein, 69626 Villeurbanne Cédex, France

Received January 3, 1994; revised March 24, 1994

A steady-state tracing kinetic study of the oxidative coupling of methane reaction at 800°C over Li^+-doped TiO_2 catalyst was performed. In particular, the carbon and oxygen reaction pathways which lead to the formation of CO_2 have been probed using $^{13}CH_4$ and $^{18}O_2$ isotope gases under reaction conditions. The results obtained indicate that there is practically no reversibly adsorbed CH_4 on the catalyst surface, while there is a very small reservoir of carbon-containing intermediate species which eventually lead to CO_2 (0.1 μmol/g). A large reservoir of oxygen species, participating in the formation of CO_2 (at least 12.0 μmol/g), was detected, while subsurface lattice oxygen species also participate in the oxygen reaction pathway to form CO_2. In addition, large amounts of inactive carbonaceous species (17.0 μmol/g) accumulate on the catalyst surface after 1 h on stream. These species do not participate in the reaction route to form CO_2 (spectator species).

INTRODUCTION

The application of steady-state tracing techniques in heterogeneous catalysis has long been appreciated as an important and valuable tool to *in situ* elucidate reaction pathways (1). In particular, quantification of surface reaction intermediate species which are in a sequence of steps, provides important insight to the assignment of possible rate-limiting step(s) in the reaction sequence (1, 2). In addition, it is also possible to determine rate constants of individual reaction steps from the measured responses based on appropriate mathematical analyses of these responses (1, 3–5). In some cases, it might also be possible to determine rate constants based only on the measured steady-state rate (TOF) and surface coverage, θ, of a given intermediate species (k = TOF/θ) (2, 6).

The steady-state tracing technique, which involves an abrupt switch from a reactant species in the feed to a corresponding isotopically labelled species, has recently found application in the investigation of the mechanism of oxidative coupling of methane (OCM) over Li/MgO, La_2O_3, and Sm_2O_3 catalysts (7–11). These studies indicated that under reaction conditions the amount of reversibly adsorbed CH_4 is practically zero, whereas there is a large reservoir of surface/subsurface oxygen species which are found in the reaction pathways of CO and CO_2 formation. In addition, the surface coverage of the precursor intermediate species which lead to C_2H_6 is also small (7, 9).

In the present work, the carbon and oxygen reaction pathways which lead to the formation of CO_2 under OCM reaction conditions were specifically investigated over 1 wt% Li_2O-doped TiO_2 catalyst. It has been found that the present catalyst formulation exhibits good activity, C_2-hydrocarbons selectivity, and stability characteristics for methane partial pressures in the range of 0.3–0.5 bar (12). Kinetic studies under OCM reaction conditions (13), as well as transient studies concerning the reactivity of CH_4, C_2H_4, and C_2H_6 with the lattice and adsorbed oxygen species of the Li^+-doped TiO_2 catalysts, have been reported previously (14, 15). These results are discussed in relation to the steady-state tracing results of the present work.

EXPERIMENTAL

(a) Preparation and Characterization of Li^+-Doped TiO_2 Catalyst

Lithium-doped TiO_2 catalyst was prepared by the method of high-temperature diffusion. Lithium nitrate was used as precursor of the doping Li^+ cation in an appropriate amount so as to yield 1 wt% lithium oxide concentration (based on $Li_2O/(Li_2O + TiO_2)$). The lithium precursor was mixed with TiO_2 (Degussa P-25) in a beaker containing distilled water. The slurry was heated under continuous stirring to evaporate the water, and the residue was further heated at 110°C overnight. The solid

0021-9517/94 $6.00

material obtained was crushed and sieved to about 48 mesh, placed in a ceramic tube and fired in air at 900°C for 6 h.

The BET surface area of the catalyst was found to be ca. 0.1 m^2/g. Other characterization measurements performed on the present catalyst, such as electrical conductivity, surface acidity and basicity, XRD, and XPS, have been reported in detail elsewhere (13).

(b) Catalyst Treatment

Before any measurements were obtained, the catalyst sample (0.41 g) was treated with oxygen at 800°C for 2 h. Between successive steady-state tracing experiments the catalyst sample was treated with oxygen at 800°C for 30 min in order to establish approximately a similar initial surface state.

(c) Flow System for Steady-State Tracing Studies

Steady-state tracing experiments were carried out in a flow system described earlier (16, 17). The isotopic composition of gases was continuously monitored at the reactor outlet by on-line mass spectrometry and gas chromatography. The steady-state tracing experiment consisted of a switch from $^{12}CH_4/^{16}O_2$/He mixture (P_{CH_4} = 0.24 bar, CH_4/O_2 = 4.4) to either $^{12}CH_4/^{18}O_2$/He or $^{13}CH_4/^{18}O_2$/He mixture, of the same methane and oxygen isotopic composition, at a flow rate of 32 ml/min (ambient). The time delay of the Argon signal from the switching valve to the mass spectrometer detector through the reactor, loaded with the catalyst sample, was 14 s. This time was subtracted from all the transient responses presented here.

The reactor used in this study was a fixed-bed quartz reactor designed to minimize void volume, after loaded with the catalyst sample (16, 17). Heating was provided by a tubular furnace. The temperature of the catalyst was measured by a *K*-type thermocouple placed at the outer surface of the reactor cell in the zone of the catalyst bed.

RESULTS

(a) Steady-State Tracing

Figure 1 shows the response of the reactor outlet composition after the switch $^{12}CH_4/^{16}O_2$/He (1h) → $^{13}CH_4/^{16}O_2$/He/Ar (300 s) → $^{12}CH_4/^{16}O_2$/He (t) at 800°C is made. Here, t designates the real time of the experiment. The results are expressed in terms of the variable Z, which represents the fraction of the ultimate change (giving Z = 1) as a function of time. Thus, Z is defined by

$$Z(t) = (y(t) - y_\infty)/(y_0 - y_\infty), \qquad [1]$$

where the subscripts 0 and ∞ refer to values of y (mole fraction) just before the switch (t = 0) and long after the switch ($t \to \infty$). Therefore, Z varies from 1 (t = 0) to 0 ($t \to \infty$). The curve labelled as Ar is the argon response as the gas passes through the reactor containing the catalyst sample. For the curve labelled $^{13}CH_4$, y represents the fraction of $^{13}CH_4$ in the gas phase at the reactor outlet. Thus, if there was no reversibly adsorbed $^{12}CH_4$ under $^{12}CH_4/^{16}O_2$/He treatment, then the $^{13}CH_4$ response would have been identical to the Ar curve. This is indeed what is observed, as indicated in Fig. 1, which shows the Ar and $^{13}CH_4$ curves to be exactly superimposed. On the other hand, the $^{13}CO_2$ response curve is above the Ar curve at all times during the transient, a result which indicates that there is an amount of carbon-containing intermediate species in the carbon pathway from CH_4 to CO_2.

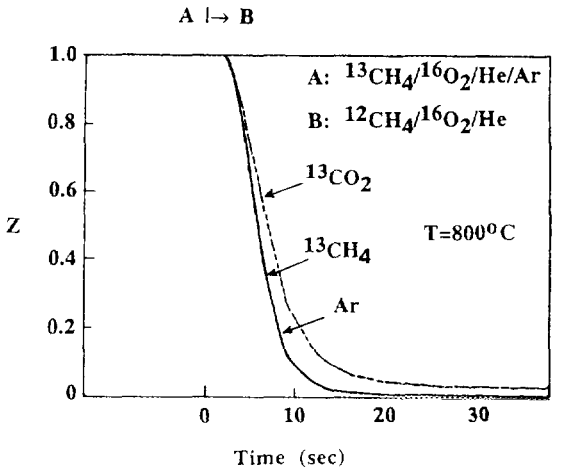

FIG. 1. Dimensionless experimental responses of Ar, $^{13}CH_4$, and $^{13}CO_2$ obtained during steady-state tracing according to the delivery sequence $^{12}CH_4/^{16}O_2$/He (1 h) → $^{13}CH_4/^{16}O_2$/He/Ar (300 s) → $^{12}CH_4/^{16}O_2$/He (t). T = 800°C, P_{CH_4} = 0.24 bar, and CH_4/O_2 = 4.4.

The $^{13}CO_2$ response which is shown in Fig. 1 reflects the transient incorporation of ^{12}C into the ^{13}C carbon-containing intermediate species pool, which eventually leads to a steady-state $^{12}CO_2$ production rate. In other words, the decay of the $^{13}CO_2$ curve represents the depletion of ^{13}C-containing intermediate species pools, the size of which and the reaction kinetics associated with them determine the shape of the $^{13}CO_2$ response curve shown in Fig. 1. The area difference between the $^{13}CO_2$ and Ar curves is proportional to the amount of carbon-containing intermediate species which are in the carbon-pathway to form CO_2. This amount is found to be 0.1 μmol/g. It is noted that after 200 s on stream in $^{12}CH_4/^{16}O_2$ the value of $Z_{^{13}CO_2}$ equals zero. At the conditions of the experiment shown in Fig. 1, the CH_4 conversion is 5.6%, the O_2 conversion is 20%, the C_2H_4/C_2H_6 ratio is 0.57, the CO/CO_2 ratio is 0.95, and the C_2-hydrocarbons selectivity is 56%.

In order to elucidate the role of subsurface lattice oxygen in the formation of CO_2, the following experiment was performed. After the catalyst was treated with the reaction mixture at 800°C for 1h, the feed was changed to $^{13}CH_4/^{18}O_2$/He for 6 min. During this time, $^{13}C^{16}O_2$, $^{13}C^{16}O^{18}O$, and $^{13}C^{18}O_2$ responses were followed by on-line mass spectrometry. At the end of the 6-min treatment with $^{13}CH_4/^{18}O_2$, the feed was changed back to $^{12}CH_4/^{16}O_2$. These results are shown in Fig. 2, where the parameter Z represents the fractional concentration of a given CO_2 isotopic species with respect to the total CO_2 concentration obtained at steady-state conditions. There is a rapid increase in the rate of formation of $^{13}C^{16}O_2$, a result not seen in the $^{13}C^{16}O^{18}O$ and $^{13}C^{18}O_2$ responses. This behaviour is discussed later. On the other hand, after 6 min of reaction under $^{13}CH_4/^{18}O_2$, there is a pseudosteady-state rate of production of $^{13}C^{16}O^{18}O$ and an increasing rate of $^{13}C^{18}O_2$ formation. The latter result is expected since, after relaxation of the transients, the Z value of $^{13}C^{18}O_2$ will be unity (steady-state production of $^{13}C^{18}O_2$ under $^{13}CH_4/^{18}O_2$ reactive atmosphere). The $^{13}C^{16}O_2$ response decays quickly, and after 5 min of the isotopic switch it reaches approximately 10% of the steady-state rate (Z = 0.1 in Fig. 2).

The ^{13}C carbon dioxide responses could be used to calculate the degree of exchange, α, of the carbon dioxide molecule with the oxygen atoms on the surface, the latter given by Equation (2),

$$\alpha = \frac{x - x_0}{x_e - x_0}, \qquad [2]$$

where x is the experimental fraction of $^{13}C^{18}O_2$, x_0 is the fraction of $^{13}C^{18}O_2$ if there were no exchange, and x_e is the fraction of $^{13}C^{18}O_2$ if all ^{16}O and ^{18}O oxygen atoms on the surface were perfectly mixed. The value of α obtained from the results of Fig. 2 is found to be in the range 0.9–1.2, suggesting the existence of a nearly statistical mixing of the oxygen atoms (^{16}O and ^{18}O) on the catalyst surface.

Integration of the $^{13}C^{16}O^{18}O$ and $^{13}C^{16}O_2$ responses obtained during the 6-min treatment with $^{13}CH_4/^{18}O_2$ mixture provides an amount of 15.0 μmol CO_2/g. This corresponds to 21.0 μmol ^{16}O/g (12 μmol ^{16}O/g corresponding to $^{13}CO_2$ and 9 μmol ^{16}O/g corresponding to $^{13}C^{16}O^{18}O$), an amount which consists part of the oxygen pool which feeds the carbon pool; the size of the carbon pool forming CO_2 was estimated earlier (Fig. 1). It is of interest to compare the amount of this oxygen to that corresponding to a monolayer. A monolayer of equivalent oxygen species is defined as the amount of oxygen (μmol/g) present on the catalyst surface. This is calculated based on the BET surface area (0.1 m^2/g), the lattice parameters, and the number of surface oxygen atoms/unit cell of rutile titania. This is found to be 1.35 μmol O_s/g. Thus, the amount of ^{16}O atoms in the oxygen pool depleted during 6 min of reaction with $^{13}CH_4/^{18}O_2$ (21.0 μmol ^{16}O/g), corresponds to about 15 monolayers of equivalent oxygen species. This result clearly demonstrates that subsurface lattice oxygen participates in the formation of CO_2 under OCM reaction conditions.

Upon switching from $^{13}CH_4/^{18}O_2$ to $^{12}CH_4/^{16}O_2$, there is a rapid decay of all three CO_2 isotopic transients towards zero (Fig. 2). This result is in harmony with the fact that the amount of active carbon species which form CO_2 is very small (see Fig. 1). During the isotopic switch $^{12}CH_4/^{16}O_2$/He → $^{13}CH_4/^{18}O_2$/He described in Fig. 2, the responses of $^{16}O_2$, $^{16}O^{18}O$, and $^{18}O_2$ were also monitored. The $^{16}O_2$ and $^{18}O_2$ responses obtained (not shown) were similar in shape to those of $^{13}C^{16}O_2$ and $^{13}C^{18}O_2$ shown in Fig. 2, respectively. However, no $^{16}O^{18}O$ signal was observed. This result is the opposite of that reported previously when the switch $^{16}O_2$/He → $^{18}O_2$/He was made at 800°C (20). For the latter experiment, there was an $^{16}O^{18}O$ transient response which indicated the exchange of ^{16}O lattice oxygen species with gaseous $^{18}O_2$. The implications of these results are discussed later.

(b) Isotopic Characterization of Carbonaceous Species Accumulated on the Catalyst Surface during Reaction

In addition to the very small amount of active carbon species accumulated on the catalyst surface after 1 h of reaction which lead to CO_2, inactive carbonaceous species may also be formed. To probe for the latter, the following experiment was performed. After reaction with $^{12}CH_4/^{16}O_2$ at 800°C for 1 h, the feed was changed to $^{13}CH_4$/He for either 30 or 120 s, followed by oxygen titra-

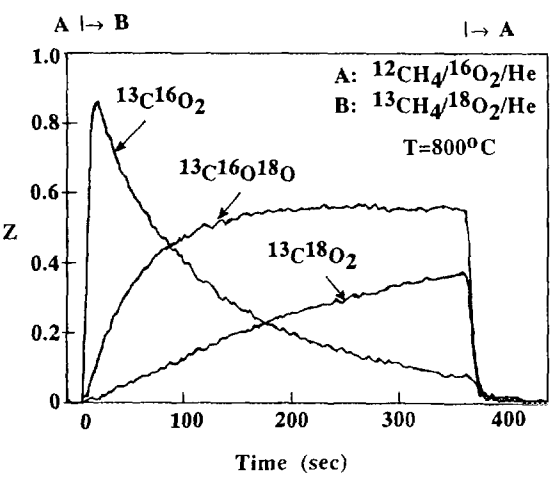

FIG. 2. Dimensionless experimental responses of $^{13}C^{16}O_2$, $^{13}C^{16}O^{18}O$, and $^{13}C^{18}O_2$ obtained during steady-state tracing according to the delivery sequence $^{12}CH_4/^{16}O_2$/He (1 h) → $^{13}CH_4/^{18}O_2$/He (360 s) → $^{12}CH_4/^{16}O_2$/He (t). T = 800°C, P_{CH_4} = 0.24 bar, and CH_4/O_2 = 4.4.

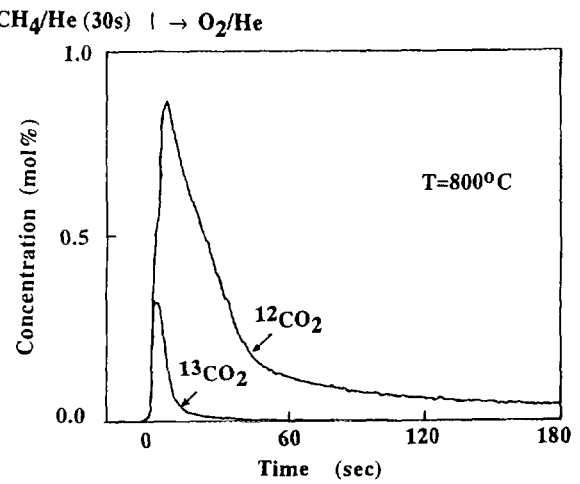

FIG. 3. Transient experimental responses of $^{12}CO_2$ and $^{13}CO_2$ obtained according to the delivery sequence $^{12}CH_4/^{16}O_2$/He (1 h) → $^{13}CH_4$/He (30 s) → O_2/He (t). T = 800°C, P_{CH_4} = 0.24 bar, and CH_4/O_2 = 4.4.

tion in O_2/He flow. The $^{12}CO_2$ and $^{13}CO_2$ species are of interest in this experiment. Figures 3 and 4 present the $^{12}CO_2$ and $^{13}CO_2$ responses obtained during oxygen titration, after 30 and 120 s of $^{13}CH_4$/He treatment, respectively. At the switch to the O_2/He mixture at 800°C, there is a rapid production of $^{12}CO_2$ as well as $^{13}CO_2$. The amount of $^{13}CO_2$ produced is found to be independent of $^{13}CH_4$/He treatment (1.6 μmol/g), whereas the opposite is true for the amount of $^{12}CO_2$ produced. There is a large decrease in the amount of $^{12}CO_2$ formed with increasing time in $^{13}CH_4$/He treatment before oxygen titration. The amount of $^{12}CO_2$ is found to be 17.0 and 6.8 μmol/g for 30 s (Fig. 3) and 120 s (Fig. 4) of $^{13}CH_4$/He treatment, respectively. It is noted that, in addition to CO_2, water is also formed during these oxygen titration experiments. Of interest is the fact that reaction(s) leading to $^{13}CO_2$ are complete within about 60 s in O_2/He flow, while longer times are required for reaction(s) leading to $^{12}CO_2$. The large amount of $^{12}CO_2$ formed in the experiment of Fig. 3, when compared to that corresponding to the steady-state tracing experiment of Fig. 1, clearly indicates that there exist on the catalyst surface carbonaceous species which are formed during reaction with CH_4/O_2 but do not participate in the reaction pathway to form CO_2. This important aspect and others arising from the results of Figs. 3 and 4 are discussed later.

(c) Nonsteady-State Experiments

Figure 5 shows transient responses of C_2H_6 and CO_2 after the switch: He → CH_4/O_2/He (t) at 800°C is made. There is a rapid increase in the rates of formation of C_2H_6 and CO_2 upon passing the reactant mixture (CH_4/O_2) over the catalyst sample, and, within about 15 s of reaction, the rates obtained correspond to 90% (Z = 0.9) of the ultimate values at steady-state (Z = 1). However, there is a slow increase in the rates towards their steady-state values after 15 s of reaction, while about 300 s are required to reach a steady-state condition. Note that the CO_2 response coincides with the C_2H_6 response for the first 15 s of the experiment, while it lags behind the C_2H_6 response for larger reaction times (Fig. 5).

Following reaction with CH_4/O_2/He/Ar for 1 h, the feed is then changed to pure He, and the transient responses of Ar and CO_2 are measured. These results are given in Fig. 6. The CO_2 response obtained lies above the Ar curve, a result which indicates that, under He purge, surface reactions take place which lead to the formation

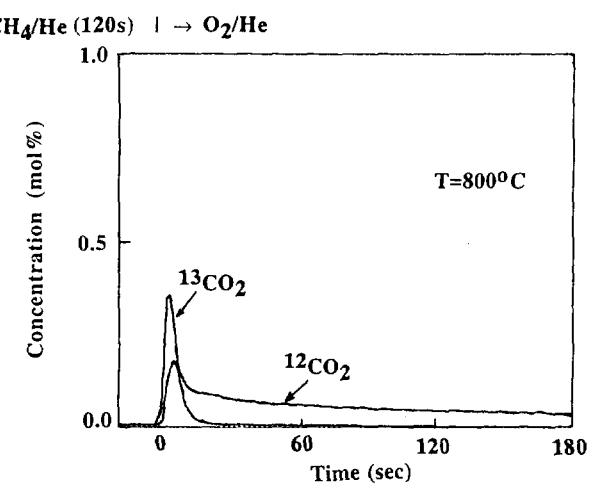

FIG. 4. Transient experimental responses of $^{12}CO_2$ and $^{13}CO_2$ obtained according to the delivery sequence $^{12}CH_4/^{16}O_2$/He (1 h) → $^{13}CH_4$/He (120 s) → O_2/He (t). T = 800°C, P_{CH_4} = 0.24 bar, and CH_4/O_2 = 4.4.

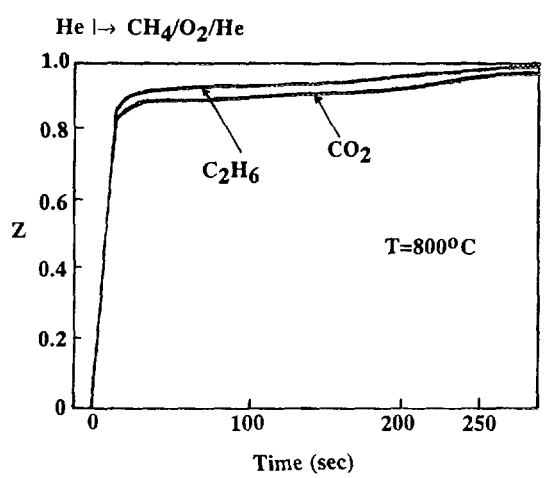

FIG. 5. Dimensionless experimental responses of CO_2 and C_2H_6 obtained according to the delivery sequence He → CH_4/O_2/He (t). T = 800°C, P_{CH_4} = 0.24 bar, and CH_4/O_2 = 4.4.

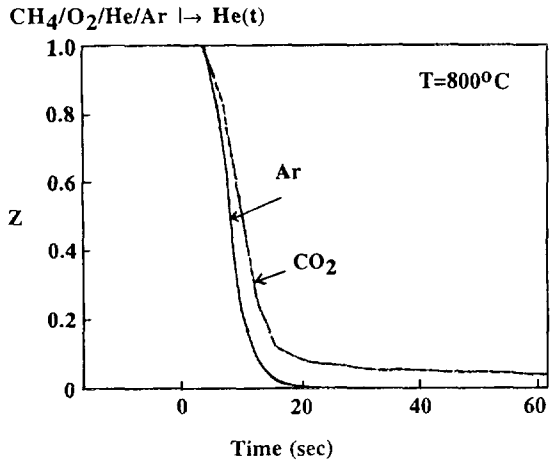

FIG. 6. Dimensionless experimental responses of Ar and CO_2 obtained according to the delivery sequence $CH_4/O_2/He/Ar$ (1 h) → He (t). T = 800°C, P_{CH_4} = 0.24 bar, and CH_4/O_2 = 4.4.

of CO_2. The amount of CO_2 produced during the 60 s of He purge is found to be 0.48 μmol/g, which is larger than that measured under the steady-state tracing experiment (Fig. 1). Longer times in He purge (10 min) at 800°C followed by O_2/He treatment (i.e., CH_4/O_2 (1 h) → He (10 min) → O_2/He (t)), resulted in no CO_2 formation, indicating that 10 min is a sufficient time to react off the surface all the carbonaceous species which can form CO_2. The implications of this result are discussed below.

DISCUSSION

(a) Steady-State Tracing: Mechanistic Aspects

An estimate of the amount of carbon-containing intermediate species which truly participate in the formation of CO_2 is made from the $^{13}CO_2$ decay curve as described in the Results section, after the switch from $^{13}CH_4/O_2$ to $^{12}CH_4/O_2$ is made (Fig. 1). This procedure is accurate if it is assumed that the exchange rate of adsorbed methane is fast compared to the reaction rate to form CO_2. For the present results this is valid since the coverage of adsorbed CH_4 is found to be practically zero (compare $^{13}CH_4$ and Ar curves in Fig. 1). Thus, the amount of all carbon-containing intermediate species which lead to CO_2 under OCM reaction conditions is of the order of 0.1 μmol/g or 1 μmol/m² (BET). This quantity is found to be smaller than that reported over other OCM catalysts. For example, Peil *et al.* (7, 8) have reported an amount of 5 μmol/g over a Sm_2O_3 catalyst at 600°C, P_{CH_4} = 0.1 bar and CH_4/O_2 = 10, and 128 μmol/g (16 μmol/m²) over a Li/MgO catalyst at 600°C, P_{CH_4} = 0.08 bar and CH_4/O_2 = 3.3. On the other hand, Lacombe *et al.* (9) reported an amount of 0.3 μmol/g (0.3 μmol/m²) over a La_2O_3 catalyst at 620°C, P_{CH_4} = 0.08 bar and CH_4/O_2 = 2, a result similar to that found in the present work. In all of the above-mentioned OCM catalytic systems, the amount of reversibly adsorbed CH_4 was found to be practically zero, as in the cases of the present Li^+-doped TiO_2, as well as on 1% Sr/La_2O_3 (11) catalysts. Thus, the mean residence time of adsorbed CH_4 in the range 600–800°C is extremely small and, therefore, not able to be measured. At lower temperatures measurable concentrations of adsorbed methane may exist over the aforementioned OCM catalytic systems.

It could be suggested that, since the surface coverage of reversibly adsorbed CH_4 species is found to be practically immeasurable, then interaction of CH_4 with the catalyst surface must proceed via an Eley–Rideal mechanism. However, a very small surface coverage of an adsorbed reaction intermediate species, which is found in a sequence of steps, could be due to a large rate constant associated with that species and reaction step. An example of this can be found in the CO/H_2 reaction. Stockwell *et al.* (18) reported that on Fe/Al_2O_3 catalyst the surface coverage of adsorbed CO was practically immeasurable, but formation of CH_4 proceeds via an adsorbed CH_x species the carbon of which is derived from the dissociation of adsorbed CO species.

The exponential-like decay response of $^{13}CO_2$ (Fig. 1) could be used to estimate the mean lifetime, τ, of the carbon-containing precursor species which form CO_2, and the rate constant, k ($k = 1/\tau$), associated with that species (6). The main assumption of this procedure is that there must be only one intermediate species in the carbon pathway from CH_4 to CO_2, or a single rate-determining step with all other steps having sufficiently high rate constants resulting in practically zero surface coverage of their respective carbon intermediate species. If we consider that a $-CH_xO$ (x = 1–3) species is likely a precursor species which forms CO_2 (19), then sequential dehydrogenation reaction steps of this CH_xO species followed by the oxidation step $CO + O_s \rightarrow CO_2$ must apply; O_s is an oxygen species, either adsorbed or lattice. Thus, the aforementioned procedure to calculate the rate constant, k, may not apply for the reaction pathway at hand. In addition, recent transient results of the reaction of C_2H_4 and C_2H_6 with lattice and adsorbed oxygen species to form CO_2 over the present catalyst suggest that part of the CO_2 formed during OCM reaction conditions may arise from combustion reactions of these C_2-hydrocarbon species (14, 15). In particular, it has been shown that a stepwise dehydrogenation mechanism of a $-CH_xO$ and/or $-CH_x$ species formed upon reaction of C_2H_4 and C_2H_6 with lattice oxygen is appropriate to explain the transient kinetic oxidation results obtained (14, 15). In addition, the C_2H_4/C_2H_6 product ratio obtained under OCM reaction conditions was in harmony with the relative reactivity of C_2H_4 and C_2H_6 toward lattice and adsorbed oxygen

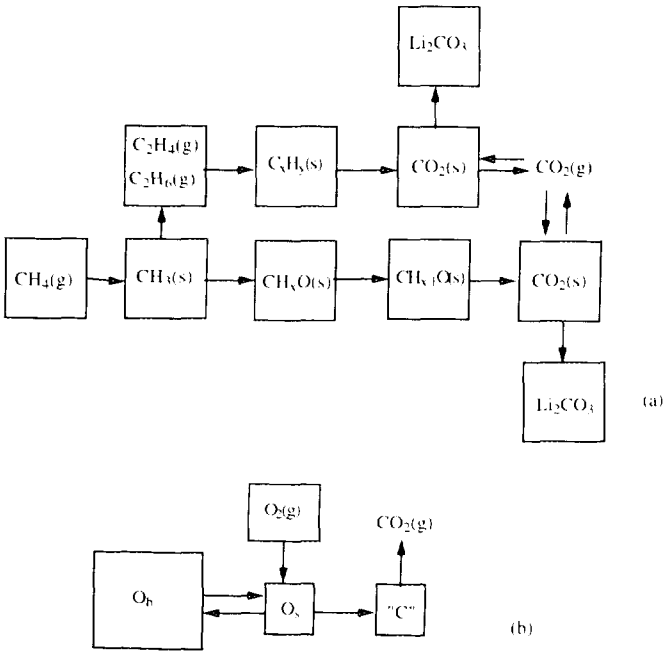

SCHEME 1. (a) CO_2 reaction pathway in OCM over Li^+-doped TiO_2 catalyst (Li_2CO_3 is an inactive (spectator) species). (b) Reversible interaction of subsurface lattice oxygen, O_b, and surface adsorbed lattice oxygen, O_s, during OCM reaction conditions, where the latter reacts with the active carbon pool "C" to eventually form CO_2 according to (a).

species (15). Based on these findings and the present results, the following mechanistic scheme (Scheme 1) for the formation of CO_2 under OCM reaction conditions is proposed:

In Scheme 1a, it is shown that gas-phase CH_4 interacts irreversibly with the surface to form methyl radicals (CH_3·) via H· abstraction, by the aid of surface oxygen species. Methyl radicals can then be oxidized to give CO_2 passing through CH_xO (x = 1–3) intermediate species. Evidence for this oxidation/dehydrogenation mechanism has been given recently over the present catalyst (14, 15). Adsorbed CO_2(s) species are also formed under steady-state OCM reaction conditions in the form of carbonate species. Methyl radicals are also the precursor species forming C_2H_6 and C_2H_4 in the gas phase, as shown in Scheme 1a; however, a surface reaction leading to C_2H_6 may not be excluded. C_2-hydrocarbons can then undergo total surface oxidation reactions to CO_2, passing through C_xH_y intermediate species, as it has been demonstrated recently (14, 15). According to the results shown in Figs. 3, 4, and 6, inactive (spectator) carbonaceous species are formed on the surface. The chemical composition of these species is proposed to be that of Li_2CO_3, as discussed in the following subsection (b).

In Scheme 1b, it is shown that gas-phase oxygen interacts irreversibly with the surface to form adsorbed oxygen species, O_s. The irreversibility of this step is supported by the results of the experiment presented in Fig. 2, in which no $^{16}O^{18}O$ signal has been detected. These results suggest that, for the present catalyst and reaction conditions, chemisorption of oxygen on the surface (i.e., oxygen vacancies) to form adsorbed oxygen species, likely O^-, must be considered as an irreversible step. Adsorbed oxygen species seem to participate in faster reaction steps, such as oxidation of carbon-containing species to CO and CO_2 and formation of –OH groups by H· abstraction from CH_4 and CH_xO species, than recombination and desorption steps leading to gaseous O_2. A similar behaviour to that described above has been observed by Lacombe *et al.* (9) over La_2O_3 and by Peil *et al.* (7) over Li/MgO catalysts. They observed that the fast isotopic equilibration of $^{16}O_2$, $^{18}O_2$, and $^{16}O^{18}O$ gases obtained in the absence of CH_4 was hindered when methane was present (CH_4/O_2 feed). Scheme 1b shows that the surface oxygen pool of O_s species interacts reversibly with a large pool of subsurface oxygen, O_b species, as evidenced by the isotopic CO_2 results of Fig. 2. In other words, the bulk of the solid feeds the surface with oxygen which, in turn, reacts with the carbonaceous pool "C" (see Scheme 1b) to form CO_2. It is noted here that the active O_s pool may be only a small fraction of the monolayer of surface lattice oxygen.

Based on the reaction Scheme 1a, the small amount of carbon-containing intermediate species measured from the steady-state tracing experiment of Fig. 1 (0.1 μmol/g) is the sum of all the intermediate species shown in the pools of Scheme 1a which lead to the formation of CO_2. Thus, the analysis of the $^{13}CO_2$ curve shown in Fig. 1 to evaluate intrinsic rate constants corresponding to given carbon species seems to be difficult.

The steady-state tracing results of Fig. 2 strongly suggest for the participation of subsurface lattice oxygen in the oxygen reaction pathway to form CO_2. The large amount of $^{13}C^{16}O_2$ produced, which accounts for about nine equivalent surface oxygen monolayers, cannot arise from any other ^{16}O source besides that of lattice oxygen in the catalyst sample. According to Scheme 1b, the large reservoir of bulk lattice oxygen, O_b, feeds the surface with ^{16}O during the isotopic transient experiment, while the latter feeds the carbon pool, "C," to eventually form CO_2. However, the isotopically labelled CO_2 species produced might interact with the surface O_s species according to the following exchange reactions:

$$C^{16}O_2 + {}^{18}O_s \leftrightharpoons C^{16}O^{18}O + {}^{16}O_s \quad [3]$$

$$C^{18}O_2 + {}^{16}O_s \leftrightharpoons C^{16}O^{18}O + {}^{18}O_s \quad [4]$$

$$C^{16}O^{18}O + {}^{16}O_s \leftrightharpoons C^{16}O_2 + {}^{18}O_s. \quad [5]$$

Thus, whatever the reaction route of forming $C^{16}O_2$ might be, it is clear that the amount of $^{13}C^{16}O_2$ response observed in Fig. 2 is a measure of the $^{16}O_s$ species able to form CO_2 under steady-state conditions. Exchange reactions [3]–[5] could only alter the quality (shape) of the $^{13}C^{16}O_2$ transient response curve shown in Fig. 2.

The present results of Fig. 2, which show the participation of subsurface lattice oxygen in the formation of CO_2, are in agreement with isotopic results recently reported (20) that have shown that a correlation between bulk lattice oxygen mobility and methane activity exists over the present Li^+-doped TiO_2 catalyst. Such a correlation has also been reported to exist over other OCM catalytic systems (21). In addition, the existence of a large pool of oxygen species which can participate in the formation of CO_2 for the present Li^+-doped TiO_2 catalyst (124 μmol/m^2 for 5 min of tracing) has also been observed over Li/MgO (7) (82 μmol/m^2 for 5 min of tracing), La_2O_3 (9), and Sm_2O_3 (11) catalysts.

The sudden increase in the rate of formation of $^{13}C^{16}O_2$ observed in Fig. 2 upon the switch from $^{12}CH_4/^{16}O_2$ to $^{13}CH_4/^{18}O_2$ might be interpreted as an indication of an Eley–Rideal interaction of gas-phase CH_4 with the catalyst surface to form CO_2. However, it is suggested that this result may be due to the very small amount of carbon species present in the pathway of CO_2 formation (Fig. 1), and also to the large value(s) of rate constant(s) associated with the rate-limiting step(s) of this pathway (Scheme 1a).

(b) Inactive (Spectator) Carbonaceous Species Formed during OCM Reaction

The transient responses of $^{12}CO_2$ shown in Figs. 3 and 4 probe for the existence of carbon-containing intermediate species which are formed on the catalyst surface under CH_4/O_2 reaction conditions but do not participate in the formation of CO_2. The formation of $^{13}CO_2$ in an amount larger than that obtained under steady-state tracing (Fig. 1) is also an important result.

During $^{13}CH_4$/He treatment of the catalyst surface, following reaction with $^{12}CH_4/^{16}O_2$, the active carbon species found in the pathway which lead to the formation of CO_2 react with surface oxygen species, in the absence of gaseous oxygen, to form CO_2. These carbon species are then replaced by ^{13}C-containing intermediate species via reaction of $^{13}CH_4$ with surface oxygen species. Thus, the interaction of CH_4 with adsorbed oxygen, the latter formed during OCM reaction, in the absence of gaseous oxygen, leads to the formation of carbonaceous species of a quantity (1.6 μmol/g) which is larger than that found in the OCM reaction pathway of CO_2 formation (Fig. 1). This result is in harmony with previous studies related to the reaction of CH_4 with lattice oxygen (14). In that study, the amount of carbonaceous species formed after CH_4/He reaction with the lattice oxygen of Li^+-doped TiO_2 was on the order of 1.0 μmol/g, while the activation energy of CO_2 formation was found to be 34 kcal/mol, to be compared with 38 kcal/mol under OCM reaction conditions. Based on these findings, it might be suggested that lattice oxygen could be considered as the primary oxidation site for CH_4 to form CO_2 under OCM reaction conditions.

On the other hand, the $^{12}CO_2$ response shown in Figs. 3 and 4 probes for the presence of a large carbon reservoir, which is formed under CH_4/O_2 at 800°C and does not participate in the formation of CO_2. The amount of these carbon species is found to decrease with increasing time in $^{13}CH_4$/He treatment (compare $^{12}CO_2$ responses in Figs. 3 and 4). The amount of these inactive carbonaceous species (about 12 monolayers of equivalent surface oxygen species) leads to certain suggestions concerning their chemical nature. As a first candidate of these inactive carbonaceous species is considered that of carbonate ion, CO_3^{2-}. Its production under the oxygen titration experiments of Figs. 3 and 4 may be explained considering the following equilibrium reactions:

$$1/2O_2(g) + O^{2-} \leftrightharpoons 2O^- \quad [6]$$

$$CO_2(g) + O^{2-} \leftrightharpoons CO_3^{2-}. \quad [7]$$

The presence of gaseous oxygen over the catalyst surface at the switch to the O_2/He mixture forces equilibrium reaction [7] towards the left, thus producing gaseous CO_2. The decrease of the amount of $^{12}CO_2$ with increasing $^{13}CH_4$/He treatment would then be understood to be due to the decomposition of CO_3^{2-} to form CO_2, since the O_2 and CO_2 are removed from the gas phase of the reactor. However, it is difficult to justify 12 equivalent monolayers of surface oxygen species to accommodate as carbonate species the amount of CO_2 obtained.

A second candidate of inactive carbonaceous species is considered that of Li_2CO_3 present as a separate phase under reaction conditions. XPS measurements performed on the 4 wt% Li_2O-doped TiO_2 catalyst after calcination (13) and before OCM reaction revealed a Li/Ti ratio of 0.42 (13). It was not possible to accurately measure the Li/Ti ratio over the present 1 wt% Li_2O-doped TiO_2 catalyst before reaction due to the weak XPS signal, likely arising from the low surface concentration of lithium. Despite this result, let us assume that, as an upper limit, the same Li/Ti ratio applies over the present catalyst. Given the BET surface area of 0.1 m^2/g and the lattice parameters of rutile TiO_2, one calculates that there exist 7.4×10^{17} Ti^{4+}/g and, therefore, 3.1×10^{17} Li/g. The latter number corresponds to 0.26 μmol Li_2CO_3/g. This number is significantly smaller than the 17.5 μmol $^{12}CO_2$/

g corresponding to the results of Fig. 3. On the other hand, the experiment of Fig. 6 applied for 10 min of He purge, followed by O_2/He treatment, resulted in no CO_2 production. This important result strongly suggests that all the inactive carbonaceous species decomposed to CO_2, during the 10 min of He treatment at 800°C, as the results of $^{12}CO_2$ response in Figs. 3, 4, and 6 also suggest. Therefore, it is logical to conclude that the inactive (spectator) carbonaceous species is Li_2CO_3 formed at reaction conditions and which decomposes under He or O_2/He treatment. What remains to be discussed is the justification of the amount of 17.5 μmol Li_2CO_3/g of catalyst with respect to the amount of 0.52 μmol surface Li^+/g of catalyst determined by XPS. As noted before, the latter number corresponds to the catalyst surface not exposed to the reaction mixture before the XPS measurements. It seems that a larger segregation of Li^+ from the bulk to the surface occurs under OCM reaction conditions resulting in the formation of a separate Li_2CO_3 phase on the surface of Li^+-doped TiO_2 catalyst. Of interest is the fact that these 17.5 μmol Li_2CO_3/g of catalyst formed correspond to only 5% of the Li_2O present in the 1 wt% Li_2O-doped TiO_2 catalyst.

In a recent publication (14), it has been shown that He treatment of CH_x or CH_xO carbonaceous species, the latter formed after reaction of C_2H_6 with the lattice oxygen of the present catalyst, did not have any effect on their subsequent oxidation reaction to CO_2 under O_2/He flow. The result of the present experiment, CH_4/O_2 (1h) $\rightarrow$ He (10 min) $\rightarrow$ O_2/He (t), where no CO_2 production has been observed during O_2/He treatment, is in agreement with what mentioned above, and the assignment to Li_2CO_3 (not to C_xH_y or CH_xO species) of the inactive carbonaceous species as discussed in the previous paragraph and also shown in Scheme 1a.

It has been recently reported (12) that the present catalyst exhibits good stability in terms of CH_4 conversion and C_2-hydrocarbons selectivity after about 8 h of operation at 900°C and for 72 h of testing. However, during the first 1 h of operation a drop in activity by three percentage units has been observed. It is likely that such deactivation is due to the accumulation of the aforementioned Li_2CO_3 phase on the surface of the Li^+-doped TiO_2 catalyst.

(c) Nonsteady-State Transient Kinetics

The transient results of Figs. 3 and 4 were obtained following first the nonsteady-state oxygen cutoff ($^{13}CH_4$/He treatment), and then the methane cutoff (O_2/He treatment), while those shown in Fig. 6 following both the methane and oxygen cutoff (He treatment) at the same time. These experiments, along with the steady-state tracing experiment of Fig. 1, reveal that a different amount of carbonaceous species leading to CO_2 is obtained, which amount strongly depends on the kind of experiment (steady-state vs nonsteady-state) applied. Of course, each quantity of carbonaceous species obtained contains its own information as already discussed in the previous sections. Goodwin and co-workers (8) have recently reported similar results over the Sm_2O_3 OCM catalytic system. However, in the nonsteady-state methane cutoff experiment the authors did not treat the catalyst with $^{13}CH_4$/He first before applying the O_2/He switch. The quantity of carbonaceous species obtained by Goodwin and co-workers (8) was larger in the case of the O_2/He switch than in the case of steady-state tracing, a result similar to that obtained in the present work.

The C_2H_6 transient response of Fig. 5 indicates that, in order for the rate of C_2H_6 production to reach its steady-state value, at least 5 min of reaction time are required since CH_4/O_2 is passed over the catalyst. This means that during this 5-min period of the transient, surface processes control the establishment of constant surface coverages of reaction intermediate species which are involved in the C_2H_6 formation. It is speculated that the inactive Li_2CO_3 phase formed may block active surface oxygen sites, O_s, which are required for $H\cdot$ abstraction from the CH_4 molecule to form CH_3 radicals and subsequently C_2H_6 by gas-phase coupling (22, 23). This explanation applies equally well for the transient behaviour of CO_2 formation shown in Fig. 5. According to Scheme 1a, active O_s species are required to form CO_2 either via a CH_xO or a C_xH_y intermediate species.

CONCLUSIONS

The following conclusions are drawn from the results of the present investigation:

1. The amount of reversibly adsorbed methane on the surface of Li^+-doped TiO_2 catalyst during OCM reaction at 800°C is practically immeasurable.

2. There is a very small (0.1 μmol/g) reservoir of carbon-containing intermediate species which truly participate in the formation of CO_2 under OCM reaction conditions.

3. There is a large (17.0 μmol/g) reservoir of carbon-containing species formed during OCM reaction which do not participate in the formation of CO_2 (spectator species). However, these carbon species are reactive under CH_4/He, O_2/He and pure He atmospheres, producing gaseous CO_2. Evidence is provided that the majority of these species must be Li_2CO_3. In addition, these species may contribute to the process of catalyst deactivation.

4. There is a large reservoir of subsurface lattice oxygen species which participate in the formation of CO_2 under OCM reaction conditions.

5. The present results, and others reported earlier (14, 15), suggest that the steady-state surface coverages of

carbon-containing intermediate species which lead to the formation of CO_2 are derived from CH_4, while C_2-hydrocarbons seem to have a minor contribution to the steady-state rate of CO_2 formation.

ACKNOWLEDGMENT

Financial support by the Commission of the European Community (Contract JOUF-0044-C) is gratefully acknowledged.

REFERENCES

1. Happel, J., "Isotopic Assessment of Heterogeneous Catalysis." Academic Press, San Diego, 1986.
2. Biloen, P., *J. Mol. Catal.* **21,** 17 (1983).
3. De Pontes, M., Yokomizo, G. H., and Bell, A. T., *J. Catal.* **104,** 147 (1987).
4. Stockwell, D. M., and Bennett, C. O., *J. Catal.* **114,** 354 (1988), and references therein.
5. Efstathiou, A. M., and Bennett, C. O., *J. Catal.* **120,** 137 (1989), and references therein.
6. Yang, C.-H., Soong, Y., and Biloen, P., *in* "Proceedings, 8th International Congress on Catalysis, Berlin, 1984," Vol. II, p. 3. Dechema, Frankfurtam-Main, 1984.
7. Peil, K. P., Goodwin, J. G., and Marcelin, G., *J. Catal.* **131,** 143 (1991).
8. Peil, K. P., Goodwin, J. G., and Marcelin, G., *J. Catal.* **132,** 556 (1991).
9. Lacombe, S., Sanchez, J. G., Delichere, P., Mozzanega, H., Tatibouet, J. M., and Mirodatos, C., *Catal. Today* **13,** 273 (1992).
10. Ekstrom, A., and Lapszewicz, J. A., *J. Am. Chem. Soc.* **110,** 5226 (1988).
11. Kalenik, Z., and Wolf, E. E., *Catal. Today* **13,** 255 (1992).
12. Papageorgiou, D., Efstathiou, A. M., and Verykios, X. E., *Appl. Catal.*, A: General **111,** 41 (1994).
13. Efstathiou, A. M., Boudouvas, D., Vamvouka, N., and Verykios, X. E., *J. Catal.* **140,** 1 (1993).
14. Efstathiou, A. M., Papageorgiou, D., and Verykios, X. E., *J. Catal.* **141,** 612 (1993).
15. Papageorgiou, D., Efstathiou, A. M., and Verykios, X. E., *J. Catal.* **147,** 279 (1994).
16. Mirodatos, C., Holmen, A., Mariscal, R., and Martin, G. A., *Catal. Today* **6,** 601 (1990).
17. Mirodatos, C., *Catal. Today* **9,** 83 (1991).
18. Stockwell, D. M., Bianchi, D., and Bennett, C. O., *J. Catal.* **113,** 13 (1988).
19. Bytyn, W., and Baerns, M., *Appl. Catal.* **23,** 199 (1986).
20. Efstathiou, A. M., Papageorgiou, D., and Verykios, X. E., *J. Catal.* **144,** 352 (1993).
21. Solokovskii, V. D., *React. Kinet. Catal. Lett.* **35,** 337 (1987).
22. Driscoll, D. J., Martir, W., Wang, J.-X., and Lunsford, J. H., *J. Am. Chem. Soc.* **107,** 58 (1985).
23. Campbell, K. D., and Lunsford, J. H., *J. Phys. Chem.* **92,** 5792 (1988).